J|A|C|S
ARTICLES
Published on Web 03/07/2003

Can the Ebselen Derivatives Catalyze the Isomerization of Peroxynitrite to Nitrate?

Djamaladdin G. Musaev,*,† Yurii V. Geletii,† Craig L. Hill,† and Kimihiko Hirao‡

Contribution from the Cherry L. Emerson Center for Scientific Computation, and Department of Chemistry, Emory University, Atlanta, Georgia 30322, and Department of Applied Chemistry, School of Engineering, The University of Tokyo, Tokyo 113-8656, Japan

Received September 20, 2002; E-mail: dmusaev@emory.edu

Abstract: The reaction of ebselen and its derivatives (**1**−**7**) with peroxynitrite anion ($ONOO^-$; PN) has been studied in gas phase and in aqueous, dichloromethane, benzene, and cyclohexane solutions using B3LYP/6-311+G(d,p)//B3LYP/6-311G(d,p) and PCM-B3LYP/6-311+G(d,p)//B3LYP/6-311G(d,p) approaches, respectively. It was shown that the reaction of **2** (R═H) with PN proceeds via **2** + PN → **2**-PN → **2**-TS1 (O−O activation) → **2**-O(NO_2^-) → **2**-SeO + NO_2^- pathway with a rate-determining barrier of 25.3 (14.8) kcal/mol at the NO_2^- dissociation step (numbers presented without parentheses are enthalpies, and those in parentheses are Gibbs free energies). The NO_3^- formation process, starting from the complex **2**-O(NO_2^-), requires by (7.9) kcal/mol more energy than the NO_2^- dissociation process and is unlikely to compete with the latter. Thus, in the gas phase, the peroxynitrite → nitrate isomerization catalyzed by complex **2** is unlikely to occur. It is shown that the NO_3^- formation process is slightly more favorably than the NO_2^- dissociation process for complex **4**, with a strongest electron-withdrawing ligand R═CF_3. Therefore, complex **4** (as well as complex **6** with R═OH) is predicted to be a good catalyst for peroxynitrite ↔ nitrite isomerization in the gas phase. Solvent effects (a) change the rate-determining step of the reaction **2** + PN from NO_2^- dissociation in the gas phase to O−O activation, which occurs with barriers of (13.9), (8.4), (8.4), and (8.2) kcal/mol in water, dichloromethane, benzene, and cyclohexane, respectively, and (b) significantly reduce the NO_2^- dissociation energy, while only slightly destabilizing the NO_3^- formation barrier, and make the peroxynitrite ↔ nitrate isomerization process practically impossible, even for complex **4**.

Introduction

Peroxynitrite anion ($ONOO^-$; PN), formed by the direct and rapid combination of nitric oxide (NO) and superoxide anion (O_2^-), is a potent cytotoxic agent and has attracted great interest over the past decades.[1] (The term peroxynitrite is used to refer to the peroxynitrite anion, O═NOO^-, and peroxynitrous acid, ONOOH, unless otherwise indicated. The IUPAC-recommended names are oxoperoxonitrate (−1) and hydrogen oxoperoxonitrate, respectively. The abbreviation PN is used to refer peroxynitrite anion O═NOO^-). The reaction

$$NO + O_2^- \leftrightarrow OONO^-$$

is a diffusion-controlled process and occurs at an average rate constant[1d,2−4] of 1.9×10^{10} M^{-1} s^{-1}, which is ∼3 times faster than the rate of superoxide scavenge by superoxide dismutase.[5] The peroxynitrite anion is stable in alkaline solution, but under physiological conditions, it quickly protonates and forms peroxynitrous acid,[4] HOONO, which undergoes rapid homolysis to give the OH and NO_2 radical pairs.[1a,6,7] Both PN and HOONO, as well as the PN-related radicals (OH, NO_2, and CO_3^- formed during the reaction of PN with CO_2 molecule[8−10]), react rapidly with numerous biomolecules, including proteins, lipids, DNA, antioxidants, and aromatic compounds.[2,11−19] It

† Emory University.
‡ The University of Tokyo.

(1) See: (a) Beckman, J. S.; Beckman, T. W.; Chen, J.; Marshall, P. A.; Freeman, B. A. *Proc. Natl. Acad. Sci. U.S.A.* **1990**, *87*, 1620. (b) Beckman, J. S.; Crow, J. P. *Biochem. Soc. Trans.* **1993**, *21*, 330. (c) Ischiropoulos, H.; Zhu, L.; Beckman, J. S. *Arch. Biochem. Biophys.* **1992**, *298*, 446. (d) Huie, R. E.; Padmaja, S. *Free Radical Res. Commun.* **1993**, *18*, 195.
(2) Beckman, J. S. The Physiological and Pathophysiological Chemistry of Nitric Oxide. In *Nitric Oxide: Principles and Actions*; Lancaster, J., Ed.; Academic Press: San Diego, CA, 1996; p 1.
(3) Kissner, R.; Nauser, T.; Bugnon, P.; Lyle, P. G.; Koppenol, W. H. *Chem Res. Toxicol.* **1998**, *11*, 557.
(4) Kissner, R.; Nauser, T.; Bugnon, P.; Lyle, P. G.; Koppenol, W. H. *Chem Res, Toxicol.* **1997**, *10*, 1285.
(5) Fielden, E. M.; Roberts, P. B.; Bray, R. C.; Lowe, D. J.; Mautner, G. N.; Rotilio, G.; Calabrese, L. *Biochem. J.* **1974**, *139*, 49.
(6) Koppenol, W. H.; Moreno, J. J.; Pryor, W. A.; Ischiropoulos, H.; Beckman, J. S. *Chem Res, Toxicol.* **1992**, *5*, 834.
(7) Pryor, W. A.; Gueto, R.; Jin, X.; Koppenol, W. H.; Ngu-Schwemlein, M.; Squadrito, G. L.; Uppu, P. L.; Uppu, R. M. *Free Radical Biol. Med.* **1995**, *18*, 75.
(8) Uppu, R. M.; Squadrito, G. L.; Pryor, W. A. *Arch. Biochem. Biophys.* **1996**, *327*, 335.
(9) (a) Lymar, S. V.; Hurst, J. K. *Inorg. Chem.* **1998**, *37*, 294. (b) Lymar, S. V.; Jiang, Q.; Hurst, J. K. *Biochemistry* **1996**, *35*, 7855.
(10) Goldstein, S.; Czapski, G. *J. Am. Chem. Soc.* **1998**, *120*, 3458.
(11) Rosen, G. M.; Freeman, B. A. *Proc. Natl. Acad. Sci. U.S.A.* **1984**, *81*, 7269.
(12) Marla, S. S.; Lee, J.; Groves, J. T. *Proc. Natl. Acad. Sci. U.S.A.* **1997**, *94*, 14243.
(13) Denicola, A.; Souza, J. M.; Radi, R. *Proc. Natl. Acad. Sci. U.S.A.* **1998**, *95*, 3566.
(14) Rachmilewitz, D.; Stamler, J. S.; Karmeli, F.; Mullins, M. E.; Singel, D. J.; Loscalzo, J.; Xavier, R. J.; Podolsky, D. K. *Gastroenterology* **1993**, *105*, 1681.
(15) Squadrito, G. L.; Jin. X.; Pryor, W. A. *Arch. Biochem. Biophys.* **1995**, *322*, 53.
(16) Lee, J.; Hunt, J. A.; Groves, J. T. *J. Am. Chem. Soc.* **1998**, *120*, 6053.
(17) Crow, J. P.; Beckman, J. S.; McCord, J. M. *Biochemistry* **1995**, *43*, 3544.

was shown that PN crosses lipid membranes at a rate significantly faster than the rates of its known decomposition pathways and travels distances of cellular dimensions, even in the presence of biological membranes. Its high reactivity with biological targets combined with its high mobility even in the presence of biological membranes implicates it in many disease states.[1,2] Therefore, it is quite important to search for the drugs that can intercept this powerful oxidizing and nitrating agent and, thus, to detoxify it. Such a strategy represents a novel therapeutic intervention in diseases associated with the overproduction of nitric oxide and superoxide.

Recently, it was shown that a series of water-soluble Fe^{III} porphyrin complexes,[20] heme-containing proteins,[21] and selenoproteins,[22] as well as synthetic organoselenium[23] (for example, ebselen (2-phenyl-1,2-benzisoselenazol-3(2*H*)-one[24]) and -sulfur (for example, methionine[25]) compounds, can intercept PN and catalyze its decomposition and isomerization or reaction with antioxidants. The elucidation of detailed mechanisms of the interception and neutralization of peroxynitrite is extremely important and will enhance our ability to search for more effective drugs for interception of this powerful oxidizing and nitrating agent. Such a task requires more comprehensive experimental and theoretical investigations.

As shown in the literature, one of the promising endogenous lines of defense against PN toxicity is ebselen[24] (Chart 1), which has been identified as an antiinflammatory agent.[26] Ebselen reacts[27] with PN at the rate constant of 2.0×10^6 M^{-1} s^{-1} and exhibits glutatione peroxidase (GPx) activity,[28] which is believed to be only reason for its peroxynitrite reduction activity (see Scheme 1). The early studies have demonstrated[27,29] that ebselen reacts with PN quantitatively and produces selenoxide as the sole selenium-containing product in alkaline pH. The main nitrogen-containing product derived from peroxynitrite in the reaction is expected to be nitrite, which should be produced in proportion to the amount of PN that reacts with ebselen. However, the recovery of nitrite was lower than expected: 40% of PN reacted with ebselen was recovered as nitrite.[29] Unfortunately, in these experiments, the nature of other nitrogen-containing products was not elucidated. One of the possible products could be nitrate, the formation of which from the peroxynitrite was experimentally demonstrated during the reaction[25] of methionine with PN. One may expect that the ebselen catalyzes the nitrate formation, which proceeds either in a concerted manner or by the stepwise (at the first step, the reaction leads to the selenoxide and nitrite and then the formed nitrite reacts with selenoxide to produce the nitrate) mechanism. In any case, if this is true, then the peroxynitrite $\leftrightarrow$ nitrate isomerization process catalyzed by ebselen could be an alternative (to its GPx activity) mechanism of ebselen's defense activity against PN toxicity. Therefore, studies of the feasibility of the $OONO^- \leftrightarrow NO_3^-$ isomerization process by ebselen are extremely important and need more detailed analysis. (It is noteworthy that the isomerization of free $OONO^-$ to NO_3^- is a highly energy demanding process and does not occur in the

Chart 1. Se Compounds Used in this Paper

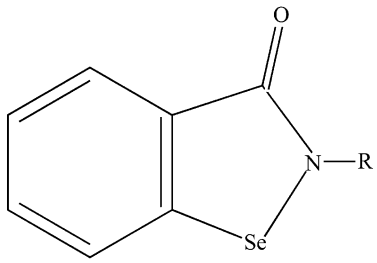

R=Ph	-	**1, Ebselen**	$R=OSiH_3$	-	**5**
R=H	-	**2**	R=OH	-	**6**
R=Me	-	**3**	$R=NH_2$	-	**7**
$R=CF_3$	-	**4**			

Scheme 1. Glutatione Peroxidase (GPx)-Type Activity of Ebselen

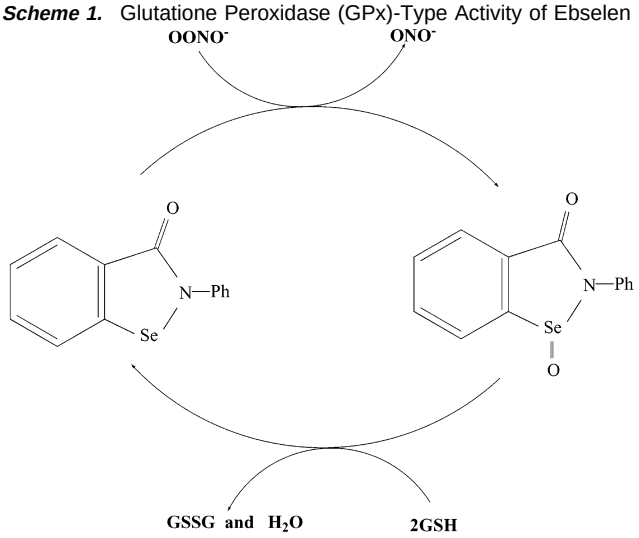

(18) Gatti, R. M.; Radi, R.; Augusto, O. *FEBS Lett.* **1994**, *348*, 287
(19) Szabo, C.; Ohshima, H. *Nitric Oxide: Biol. Chem.* **1997**, *1*, 373.
(20) (a) Stern, M. K.; Jensen, M. P.; Kramer, K. *J. Am. Chem. Soc.* **1996**, *118*, 8735. (b) See ref 16. (c) Crow, J. P. *Arch. Biochem. Biophys.* **1999**, *371*, 41. (d) See ref 12. (e) Lee, J.; Hunt, J. A.; Groves, J. T. *Bioorg. Med. Chem. Lett.* **1997**, *7*, 2913. (f) Hunt, J. A.; Lee, J.; Groves, J. T. *Chem. Biol.* **1997**, *4*, 845. (g) Crow, J. P. *Free Radical Biol. Med.* **2000**, *28*, 1487. (h) Balavoine, G. G. A.; Geletti, Y. V.; Bejan, D. *Nitric Oxide*: *Biol. and Chem.* **1997**, *1*, 507. (i) Shimanovich, R.; Hannah, S.; Lynch, V.; Gerasimchuk, N.; Mody, T. D.; Magda, D.; Sessler, J.; Groves, J. T. *J. Am. Chem. Soc.* **2001**, *123*, 3613. (j) Zhang, X.; Busch, D. H. *J. Am. Chem. Soc.* **2000**, *122*, 1229. (k) Salvemini, D.; Wang, Z. Q.; Stern, M.; Currie, M. G.; Misko, T. *Proc. Natl. Acad. U.S.A.* **1998**, *95*, 2659.
(21) (a) Floris, R.; Piersma, S. R.; Yang, G.; Jones, P.; Wever, R. *Eur. J. Biochem.* **1993**, *215*, 767. (b) Kondo, H.; Takahashi, M.; Niki, E. *FEBS Lett.* **1997**, *413*, 236. (c) Exner, M.; Herold, S. *Chem Res, Toxicol.* **2000**, *13*, 287. (d) Squadrito, G. L.; Pryor, W. A. *Chem Res. Toxicol.* **1997**, *11*, 718. (e) Radi, R. *Chem Res. Toxicol.* **1998**, *11*, 720. (f) Minetti, M.; Scorza, G.; Pietraforte, D. *Biochemistry* **1999**, *38*, 2078. (g) Herold, S.; Matsui, T.; Watanabe, Y. *J. Am. Chem. Soc.* **2001**, *123*, 4085. (h) Bourassa, J. L.; Ives, E. P.; Marqueling, A. L.; Shimanovich, R.; Groves, J. T. *J. Am. Chem. Soc.* **2001**, *123*, 5142.
(22) *Selenium in Biology and Human Health*; Burk, R. F., Ed.; Springer-Verlag: New York, 1994 and references therein.
(23) (a) Mugesh, G.; Singh, H. B. *Chem. Soc. Rev.* **2000**, *29*, 347. (b) Mugesh, G.; Panda, A.; Singh, H. B.; Punekar, N. S.; Butcher, R. J. *J. Am. Chem. Soc.* **2001**, *123*, 839. (c) Mugesh, G.; du Mont, W. W.; Sies, H. *Chem. Rev.* **2001**, *101*, 2125 and references therein. (d) Briviba, K.; Roussyn, I.; Sharov, V. S.; Sies, H. *Biochem. J.* **1996**, *319*, 13.
(24) Sies, H.; Masumoto, H. *Adv. Pharmacol.* **1997**, *38*, 2229 and references therein.
(25) Perrin, D.; Koppenel, W. H. *Arch. Biochem. Biophys.* **2000**, *377*, 266.
(26) (a) Cadenas, E.; Wefers, H.; Muller, A.; Brigelius, R.; Sies, H. In *Agents and Actions Supplements*; Parnham, M. J., Winkelmann, J., Eds.; Birkhauser-Verlag: Basel, 1982; Vol. 11, p 203. (b) Parnham, M. J.; Leyck, S.; Dereu, N.; Winkelmann, J.; Graf, E. *Adv. Inflammation Res.* **1985**, *10*, 397. (c) Wendel, A.; Tiegs, G. *Biochem. Pharmacol.* **1986**, *35*, 2115. (d) Kuhl, P.; Borbe, H. O.; Fischer, H.; Romer, A.; Safayhi, H. *Prostaglandins* **1986**, *31*, 1029. (e) Parnham, M. J.; Graf, E. *Biochem. Pharmacol.* **1987**, *36*, 3095.
(27) Masumoto, H.; Kissner, R.; Koppenol, W. H.; Sies, H. *FEBS Lett.* **1996**, *398*, 179.
(28) (a) Epp, O.; Ladenstein, R.; Wendel, A. *Eur. J. Biochem.* **1983**, *133*, 51. (b) Ren, B.; Huang, W.; Akesson, B.; Ladenstein, R. *J. Mol. Biol.* **1997**, *268*, 869. (c) Muller, A.; Cadenas, E.; Graf, P.; Sies, H. *Biochem. Pharmacol.* **1984**, *33*, 3235. (d) Wendel, A.; Fausel, M.; Safayhi, H.; Tiegs, G.; Otter, R. *Biochem. Pharmacol.* **1984**, *33*, 3241. (e) Sies, H. *Free Radical Biol. Med.* **1993**, *14*, 313. (f) Schewe, T. *Gen. Pharmacol.* **1995**, *26*, 1153.
(29) Masumoto, H.; Sies, H. *Chem Re. Toxicol.* **1996**, *9*, 262.

Table 1. Relative Energies (in kcal/mol, Relative to the Reactants, Complex **2**, and *cis*-$OONO^-$) of the Obtained Intermediates, Transition States, and Products of Reaction **2** + PN, Calculated at the B3LYP/6-311G(d,p) and B3LYP/6-311+G(d,p)//B3LYP/6-311G(d,p) Levels of Theory

	6-311G**				6-311+G**		
structures[a]	ΔE	ΔE+ZPC	ΔH	ΔG	ΔE	ΔH^b	ΔG^b
$OONO^-$, cis	0.0	0.0	0.0	0.0	0.0	0.0	0.0
$OONO^-$, ts	28.6	27.4	27.4	27.3	27.1	25.9	25.8
$OONO^-$, trans	4.6	4.2	4.3	4.3	3.4	3.1	3.1
2 + *cis*-$OONO^-$	0.0	0.0	0.0	0.0	0.0	0.0	0.0
2-PN-*cis*−*cis*	−34.1	−33.2	−33.0	−21.6	−25.3	−24.2	−12.8
2-PN-*cis*−*trans_1*	−42.1	−41.1	−40.9	−30.8	−32.2	−31.0	−20.9
2-PN-*cis*−*trans_2*	−42.6	−41.7	−41.5	−30.2	−32.5	−31.4	−20.1
2-PN-*trans*−*trans_1*	−38.8	−38.0	−37.7	−26.2	−29.5	−28.4	−16.9
2-PN-*trans*−*trans_2*	−39.3	−38.5	−38.3	−26.9	−30.1	−29.1	−17.7
2-TS1-*cis*−*cis*	−19.4	−19.3	−19.4	−7.3	−11.5	−11.5	0.6
2-TS1-*cis*−*trans*	−34.6	−34.6	−34.5	−22.7	−25.1	−25.0	−13.2
2-TS1-*trans*−*trans*	−27.8	−28.1	−28.0	−16.4	−20.8	−21.0	−9.4
2-O(NO_2)-*cis*−*cis*	−65.0	−64.2	−63.8	−52.4	−58.2	−57.0	−45.6
2-O(NO_2)-*cis*−*trans*	−63.5	−62.7	−62.3	−51.5	−58.0	−56.8	−46.0
2-O(NO_2)-*trans*−*trans*	−61.5	−60.8	−60.1	−48.1	−55.7	−54.3	−42.3
2-O(NO_2)_*with_N*	−58.6	−57.4	−57.1	−46.0	−53.7	−52.2	−41.1
2-TS2(*cis*−*cis*→ *cis*−*trans*)	−58.8	−58.4	−58.3	−46.5	−52.7	−52.2	−40.4
2-TS2(*trans*−*trans*→ *with_N*)	−54.7	−53.7	−53.6	−42.1	−50.4	−49.3	−38.3
2-TS3_NO_3^-	−39.9	−39.9	−39.6	−29.0	−34.2	−33.9	−23.3
2-NO_3^-	−83.3	−80.7	−80.7	−69.4	−74.9	−72.3	−61.0
2 + NO_3^-	−55.1	−53.3	−53.6	−53.1	−54.2	−52.7	−52.2
2-SeO + NO_2^-	−25.5	−25.7	−25.4	−25.1	−31.6	−31.5	−31.2

[a] Structures are given in Figures 1−5. [b] The zero-point energy, temperature, and entropy corrections were evaluated at the B3LYP/6-311G(d,p) level and added to the final B3LYP/6-311+G(d,p) energetics.

modest conditions.[9]) Furthermore, the existing experiments do not provide information about the geometries and energetics of the reactants, expected intermediates, transition states and products, and factors (electronic, steric, solvent) affecting to the mechanism of the reaction of ebselen with PN. These data are also important in the search for better antioxidants for PN.

Therefore, the goal of this paper is to elucidate the mechanisms and the factors (such as electronic, steric, and solvent effects) affecting the mechanisms of reaction of ebselen and its derivatives with PN. Here we plan the following: (a) to elucidate the geometrical and electronic structures, as well as the energetics of the assumed intermediates and transition states of the reaction of ebselen and its derivatives with PN, (b) to analyze the mechanism and the factors affecting both the peroxynitrite ↔ nitrate isomerization and selenoxide and nitrite formation (which is the first step of its GPx activity) processes, and (c) to check the feasibility of ebselen (and its derivatives) as catalysts for the peroxynitrite ↔ nitrate isomerization process.

Calculation Procedures

All calculations were performed with quantum chemical package Gaussian-98.[30] The geometries, vibrational frequencies, and energetics all structures were calculated using hybrid density functional theory, B3LYP.[31] In these calculations, we used two types of basis sets: 6-311G(d,p) and 6-311+G(d,p). Our benchmark studies of the geometries of several intermediates and reactants of the reaction of complex **2** (see Chart 1) with PN at the B3LYP/6-311G(d,p) and B3LYP/6-311+G(d,p) levels show that diffuse function is not important for the geometry calculations (see Figures 1, 2, and 4). Therefore, below we will report only B3LYP/6-311G(d,p) optimized geometries and vibrational frequencies for all structures (see Chart 1). Meantime, our studies revealed that the diffuse function is crucial for the calculations of relative energies (see Table 1), especially for the steps involving $ONOO^-$ coordination and NO_2^- and NO_3^- dissociation. For these steps, the inclusion of a diffuse function could reduce the B3LYP/6-311G(d,p) calculated energies by up to 10 kcal/mol. Therefore, below we will discuss only the B3LYP/6-311+G(d,p) energetics calculated at the B3LYP/6-311G(d,p) optimized geometries for all located structures (below, this approach is denoted as B3LYP/6-311+G(d,p)//B3LYP/6-311G(d,p)), unless otherwise stated. Previous studies[32] on the structure and stabilities of *cis*- and *trans*-peroxynitrite anion, as well as their hydrated forms, show that the B3LYP and more sophisticated CCSD(T), G2, and CBS-Q approaches using the 6-311+G(d,p) basis sets provide a very close agreement. Meantime, we[33] and others[34] have demonstrated that the B3LYP/6-311+G(d,p) approach underestimates the calculated energetic barriers ∼5 kcal/mol compared to the CCSD(T) and QCISD(T) methods. Since in this paper we discuss relative energies calculated at the same (B3LYP/6-311+G(d,p)) level of theory, we believe that any underestimation of the calculated barriers by the B3LYP method will not affect our general conclusions.

To analyze the solvent effects we have performed single-point polarizable continuum model[35] calculations at the B3LYP/6-311G(d,p) optimized geometries using 6-311+G(d,p) basis sets, named below as PCM-B3LYP/6-311+G(d,p). As a solvent we used water, dichloro-

(30) Frisch, M. J.; Trucks, G. W.; Schlegel, H. B.; Scuseria, G. E.; Robb, M. A.; Cheeseman, J. R.; Zakrzewski, V. G.; Montgomery, J. A., Jr.; Stratmann, R. E.; Burant, J. C.; Dapprich, S.; Millam, J. M.; Daniels, A. D.; Kudin, K. N.; Strain, M. C.; Farkas, O.; Tomasi, J.; Barone, V.; Cossi, M.; Cammi, R.; Mennucci, B.; Pomelli, C.; Adamo, C.; Clifford, S.; Ochterski, J.; Petersson, G. A.; Ayala, P. Y.; Cui, Q.; Morokuma, K.; Malick, D. K.; Rabuck, A. D.; Raghavachari, K.; Foresman, J. B.; Cioslowski, J.; Ortiz, J. V.; Baboul, A. G.; Stefanov, B. B.; Liu, G.; Liashenko, A.; Piskorz, P.; Komaromi, I.; Gomperts, R.; Martin, R. L.; Fox, D. J.; Keith, T.; Al-Laham, M. A.; Peng, C. Y.; Nanayakkara, A.; Gonzalez, C.; Challacombe, M.; Gill, P. M. W.; Johnson, B.; Chen, W.; Wong, M. W.; Andres, J. L.; Gonzalez, C.; Head-Gordon, M.; Replogle, E. S.; Pople, J. A. *Gaussian 98*, *Revision A.7*, Gaussian, Inc., Pittsburgh, PA, 1998.
(31) (a) Becke, A. D. *Phys. Rev. A* **1988**, *38*, 3098. (b) Lee, C.; Yang, W.; Parr, R. G. *Phys. Rev. B* **1988**, *37*, 785. (c) Becke, A. D. *J. Chem. Phys.* **1993**, *98*, 5648.
(32) (a) Tsai, H. H.; Hamilton, T. P.; Tsai, J. H. M.; Van der Woerd, M.; Harrison, J. G.; Jablonsky, M. J.; Beckman, J. S.; Koppenol, W. H. *J. Phys. Chem.* **1996**, *100*, 15087. (b) Tsai, J. H. M.; Harrison, J. G.; Martin, J. C.; Hamilton, T. P.; Van der Woerd, M.; Jablonsky, M. J.; Beckman, J. S. *J. Am. Chem. Soc.* **1994**, *116*, 4115.
(33) Musaev, D. G.; Hirao, K. *J. Phys. Chem.* A, in press.
(34) (a) Bach, R. D.; Gluhkovtsev, M. N.; Canepa, C. *J. Am. Chem. Soc.* **1998**, *120*, 775. (b) Lynch, B. J.; Fast, P. L.; Harris, M.; Truhlar, D. G. *J. Phys. Chem. A* **2000**, *104*, 4811.

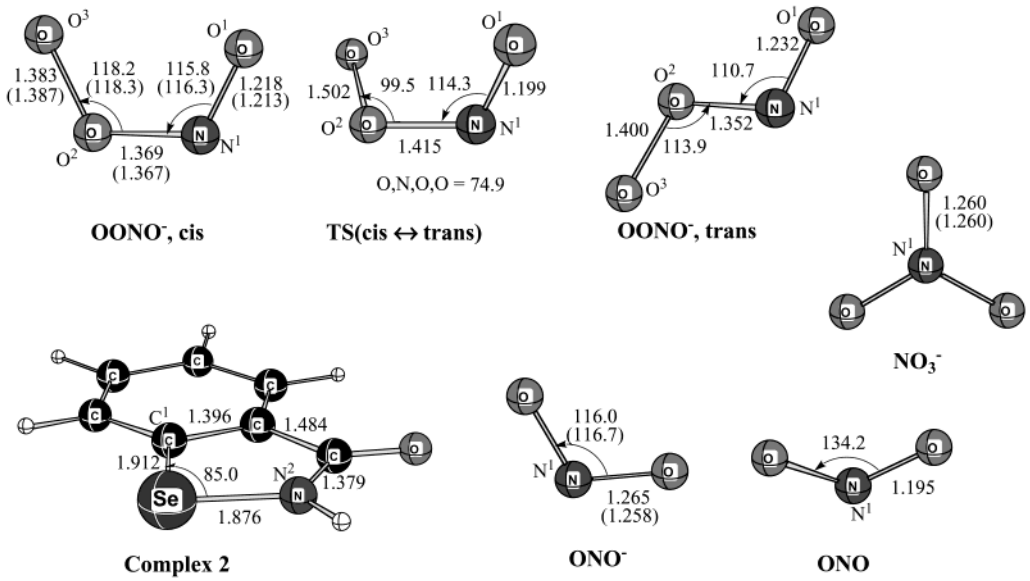

Figure 1. Calculated important geometries (distances in Å, angles in deg) of the reactants (cis and trans forms of $OONO^-$, the transitition states separating these isomers, and complex **2**), as well as expected nitrogen-containing products (molecules NO_2^-, NO_2, and NO_3^-) of the reaction **2** + PN. Data presented without parentheses were obtained at the B3LYP/6-311G(d,p) level, while those given in the parentheses were obtained at the B3LYP/6-311+G(d,p)level. The full geometrical parameters of these species are given in the Table S1 of the Supporting materials.

methane, benzene, and cyclohexane. The default dielectric constants of these solvents were taken from the Gaussian program.

Results and Discussion

This paper is organized as follows. First, we discuss the mechanism of the reaction **2** + PN in the gas phase. Here, we (a) discuss the geometrical structures and energetics of the reactants, intermediates, transition states, and products of the reaction; (b) analyze the mechanisms of the both peroxynitrite ↔ nitrate isomerization and the selenoxide and nitrite formation processes; and (c) check the feasibility of the peroxynitrite ↔ nitrate isomerization process catalyzed by **2**. In the next two sections, we elucidate the roles of electronic and solvent effects, respectively. Conclusions are given in the last section.

Reaction of 2 with $OONO^-$. First, let us discuss the reactants, $ONOO^-$ and complex **2**. The calculated geometries of the $ONOO^-$, complex **2**, and possible nitrogen-containing products of the reaction are given in Figure 1. Their energetics are presented in Table 1.

$ONOO^-$ has been the subject of many previous theoretical studies.[32,36] In general, it was found that PN has two different isomers, cis and trans, between which the cis isomer is reported to be 2-4 kcal/mol more stable than the trans isomer. These isomers are separated by a 21−27 kcal/mol barrier corresponding to the rotation around the ON−OO bond. Our data presented in Table 1 are consistent with those from the previous studies: we have found that cis isomer lies by 3.1 (3.1) kcal/mol lower than the trans isomer and is separated from the latter by 25.9 (25.8) kcal/mol barrier, calculated from the cis isomer. Note, here and below, energies given without parentheses are relative enthalpies, ΔH, while those given in parentheses are relative Gibbs free energies, ΔG, including zero-point energy, temperature, and entropy corrections. Note, the zero-point energy, temperature, and entropy corrections were calculated at the B3LYP/6-311G(d,p) level and added to the B3LYP/6-311+G(d,p) calculated energetics (see Table 1).

As seen from Figure 1, complex **2**, which is the simplest ebselen derivative, is a planar molecule with strong Se−C^1 and Se−N^2 bonds. The calculated Se−C^1 and Se−N^2 bond distances are 1.912 and 1.876 Å, respectively.

2-PN Complexes. As could be expected from the charge distributions (see Table S3 in the Supporting Information), the first step of the reaction is the coordination of the negatively charged O^3 end of PN to the positively charged Se center, to form a **2**-PN complex. Since, PN has two different isomers, cis and trans, each of them could coordinate to the Se center of **2** via two different orientations, cis and trans, to the Se−N^2 bond, and form of various isomers, such as cis−cis, cis−trans, trans−cis, and trans−trans. Here, the first definition stands for the isomer of PN, and the second definition stands for the position where PN coordinates (see Figure 2). Furthermore, each of these isomers may have several additional forms, which could be classified by the rotation of $O^1N^1O^2$ unit around the O^2−O^3 bond.

We have studied three isomers corresponding to the coordination of *cis*-PN to complex **2**, namely, the cis−cis and cis−trans_1 and cis−trans_2 isomers (Figure 2). As seen in Table 1, cis−trans_1 and cis−trans_2 isomers are degenerate: the energy difference between them is only 0.5−0.7 kcal/mol. Their main geometrical parameters are almost the same too (see Table S1 of the Supporting Information). Therefore, below, we discuss only **2**-PN-*cis*−*trans_1*. As seen from Table 1, the **2**-PN-*cis*−*trans_1* isomer is more stable than the cis−cis isomer by 6.8 (8.1) kcal/mol. The lower stability of the cis−cis isomer could be explained by the existence of the strong trans effect from the Se−C^1 bond compared to Se−N^2 in the cis−trans complex.

(35) (a) Miertus, S.; Scrocco, E.; Tomasi, J. *Chem. Phys.* **1981**, *55*, 117. (b) Miertus, S.; Tomasi, J. *Chem. Phys.* **1982**, *65*, 239. (c) Cossi, M.; Barone, V.; Cammi, R.; Tomasi, J. *Chem. Phys. Lett.* **1996**, *255*, 327. (d) Cances, M. T.; Mennucci, V.; Tomasi, J. *J. Chem. Phys.* **1997**, *107*, 3032. (e) Barone, V.; Cossi, M.; Tomasi, J. *J. Comput. Chem.* **1998**, *19*, 404.

(36) (a) Liang, B.; Andrews, L. *J. Am. Chem. Soc.* **2001**, *123*, 9848. (b) Bartberger, M. D.; Olson, L. P.; Houk, K. N. *Chem Res. Toxicol.* **1998**, *11*, 710. (c) Houk, K. N.; Condroski, K. R.; Pryor, W. A. *J. Am. Chem. Soc.* **1996**, *118*, 13002. (d) Yang, D.; Tang, Y. C.; Chen, J.; Wang, X. C.; Bartberger, M. D.; Houk, K. N.; Olson, L. *J. Am. Chem. Soc.* **1999**, *122*, 11976.

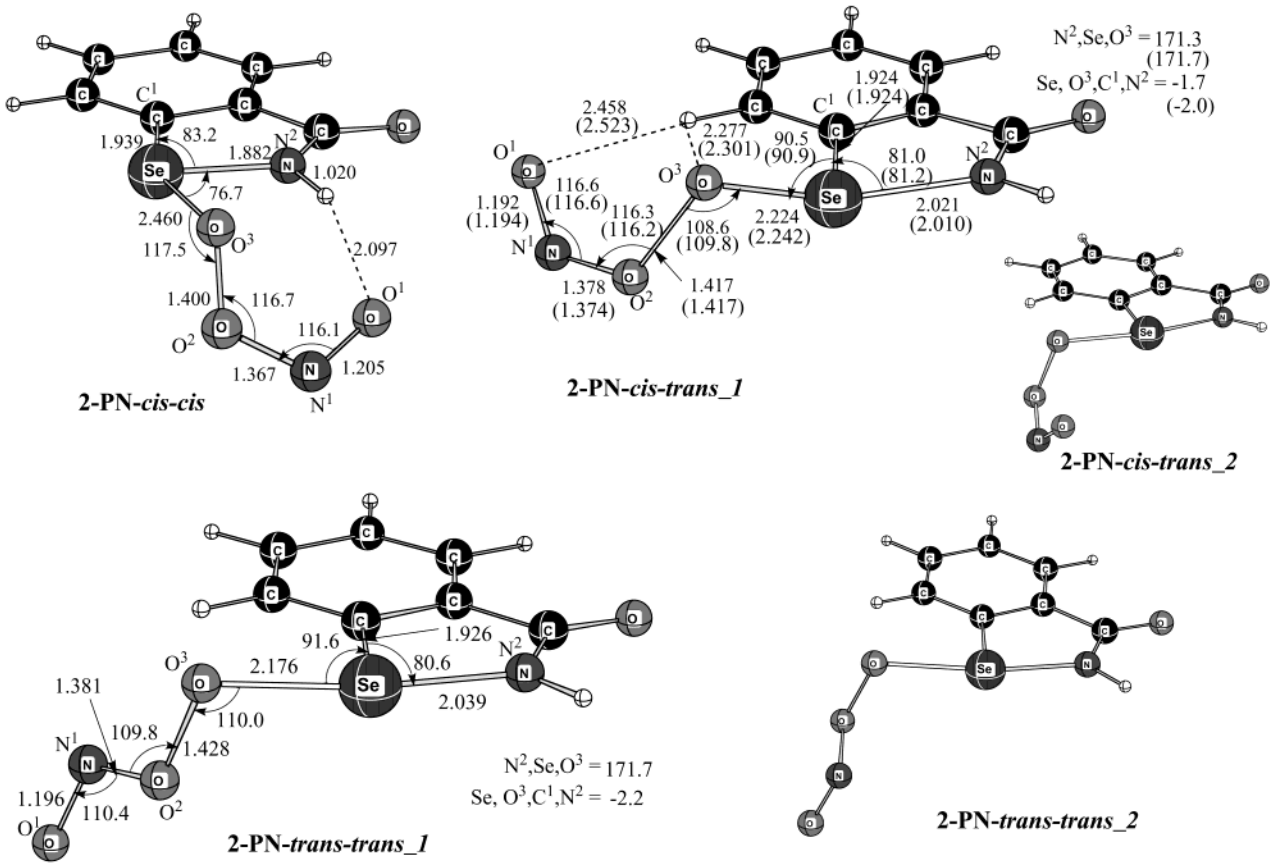

Figure 2. Calculated important geometrical parameters (distances in Å, angles in deg) of the isomers of **2**-PN complex.

This is also the reason for the longer Se−O^3 bond distance in the cis−cis isomer, 2.384 Å, than in the cis−trans_1, 2.224 Å. These energy and geometrical data for **2**-PN-*cis*−*cis* and **2**-PN-*cis*−*trans* isomers are correlated with other obtained geometrical changes, especially with the elongation of Se−N^2 and Se−C^1 bonds upon coordination of *cis*-PN to **2**. Indeed, as seen in Figure 2, in **2**-PN-*cis*−*trans_1*, the Se−N^2 bond distance elongated, by 0.145 Å, compared with that in the free complex **2**, while this effect is insignificant in **2**-PN-*cis*−*cis*. Meantime, the coordination of *cis*-PN to complex **2** only slightly changes the Se−C^1 bond distance. These geometrical changes clearly indicate that in complex **2** the Se−N^2 bond is much weaker than the Se−C^1 bond.

Since the cis coordination of *cis*-PN to the Se center is energetically less favorable than its trans coordination, for the *trans*-PN, we have studied only its trans coordination mode leading to two different isomers **2**-PN-*trans*−*trans_1* and **2**-PN-*trans*−*trans_2*. As seen in Table 1, they are are again degenerate with energy difference of ∼0.7 kcal/mol. Their main geometrical parameters are also very close, and again only one of them, isomer PN-*trans*−*trans_1*, will be discussed below. As seen in Figure 2, in PN-*trans*−*trans_1* the Se−N^2 bond is again significantly elongated, by 0.169 Å compared to the free complex **2**.

As expected, coordination of PN to complex **2** also changes the geometry of the $OONO^-$ unit. However, these changes are insignificant with a larger change in O^3−O^2 bond distance, which is elongated by 0.017, 0.034, and 0.045 Å in the complexes **2**-PN-*cis*−*cis*, **2**-PN-*cis*−*trans_1* and **2**-PN-*trans*−*trans_1*, respectively, compared with free PN.

Thus, coordination of *cis*- and *trans*-PN to complex **2** leads to formation of numerous isomers, which can easily rearrange to each other with very small rotational barriers (which were not calculated, because their role in the overall reaction mechanism is thought to be negligible). Among the isomers corresponding to the coordination of *cis*- and *trans*-PN, the **2**-PN-*cis*−*trans_1* and **2**-PN-*trans*−*trans_1* are energetically lowest, respectively. The calculated energies of the reaction **2** + PN → **2**-PN are 31.0 (20.9) and 28.4 (16.9) kcal/mol for formation of **2**-PN-*cis*−*trans_1* and **2**-PN-*trans*−*trans_1*, respectively. In other words, the cis−trans isomerization energy of the coordinated PN, 2.6 (4.0) kcal/mol, is only slightly different from that for the free PN, 3.1 (3.1) kcal/mol, reported above.

Transition States for the O−O Bond Cleavage. In the next stage of the reaction, the O^3−O^2 bond cleavage takes place via the transition states **2**-TS1-*cis*−*cis*, **2**-TS1-*cis*−*trans*, and **2**-TS1-*trans*−*trans* (Figure 3). Each of these transition states was positively characterized and has only one imaginary frequency (396i, 232i, and 148i cm^{-1}, respectively) corresponding to the O−O cleavage. Intrinsic reaction coordinate[37] (IRC) calculations show that these transition states are connected to the corresponding complexes **2**-PN-*cis*−*cis*, **2**-PN-*cis*−*trans*, and **2**-PN-*trans*−*trans*, respectively. In these transition states (Figure 3), the broken O^3−O^2 bond distances are elongated by 0.385, 0.446, and 0.496 Å, while the formed Se−O^3 and N^1−O^2 bond distances are shortened by 0.472, 0.403, and 0.401 Å and by 0.096, 0.107, and 0.082 Å, compared with the corresponding

(37) (a) Gonzalez, C.; Schlegel, H. B. *J. Chem. Phys.* **1989**, *90*, 2154. (b) Gonzalez, C.; Schlegel, H. B. *J. Phys. Chem.* **1990**, *94*, 5523.

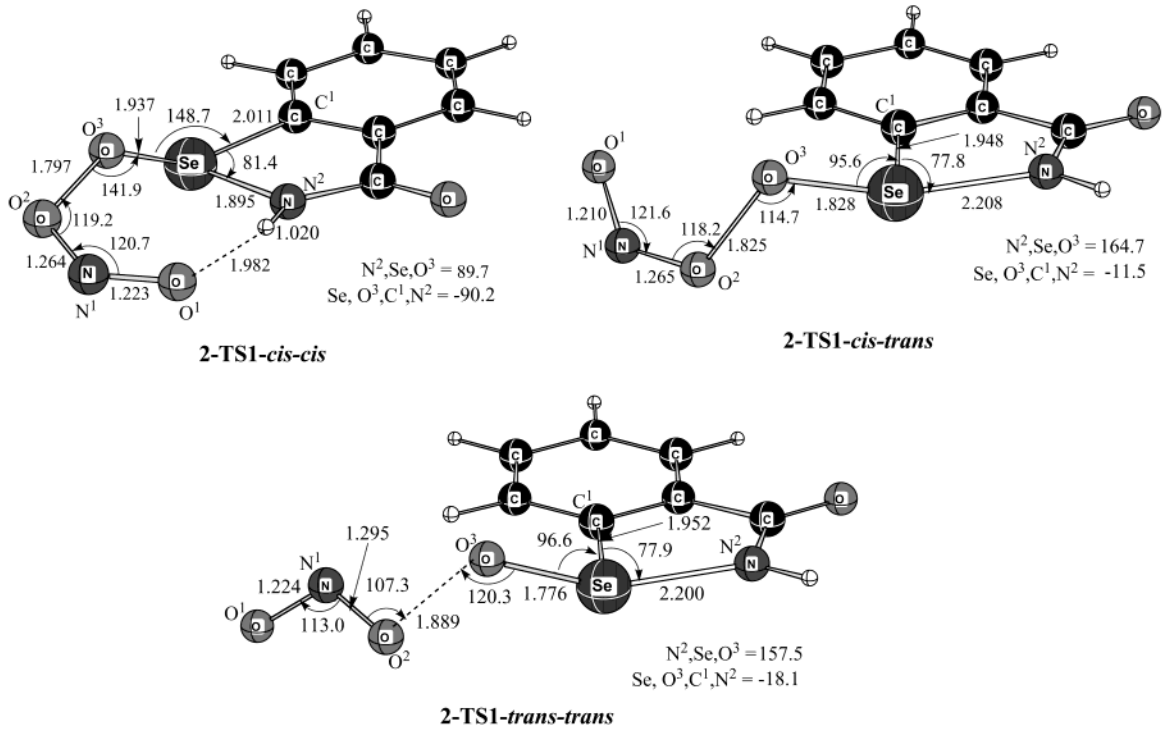

Figure 3. Calculated important geometrical parameters (distances in, Å, angles in deg) of various transition states corresponding to the O−O bond activation of the $OONO^-$ by complex **2**.

prereaction complexes **2**-PN-*cis*−*cis*, **2**-PN-*cis*−*trans*, and **2**-PN-*trans*−*trans*, respectively. All these geometrical changes are consistent with the nature of these transition states, where the O^3-O^2 bond cleavage and the $Se-O^3$ and $N^1=O^2$ double bond formation occurs. Since during this process the strong $Se-O^3$ bond is formed, the $Se-C^1$ and $Se-N^2$ bonds located trans to the formed $Se-O^3$ bond are elongated significantly.

The calculated activation barriers from the prereaction complexes **2**-PN-*cis*−*cis*, **2**-PN-*cis*−*trans*, and **2**-PN-*trans*−*trans* are 12.7 (13.4), 6.0 (7.7), and 7.4 (7.5) kcal/mol, respectively.

Note that we are aware of the existence of several different O−O activation transition states connected to the numerous isomers of the **2**-PN complex, discussed above. However, we do not expect these transition states will be significantly different from those discussed in this section either energetically or geometrically and therefore can be ignored.

It is noteworthy that the O−O bond cleavage by **2** can be considered to be a heterolytic process similar to O-atom transfer, which is common in organometallic chemistry.[38]

Products of the O−O bond cleavage are complexes **2**-O(NO_2)-*cis*−*cis*, **2**-O(NO_2)-*cis*−*trans*, and **2**-O(NO_2)-*trans*−*trans*, respectively (see Figure 4). The connectivity of these products with the corresponding transition states, **2**-PN-*cis*-*cis*, **2**-PN-*cis*−*trans*, and **2**-PN-*trans*−*trans*, has been confirmed by the IRC calculations.

In all of these isomers, the $Se=O^3$ double bond, with bond distances ranging from 1.651 to 1.654 Å, is located out of the Se(C_6H_4CONH) plane with the $\angle C^1SeO^3$ and $\angle N^2SeO^3$ angles of 104.0°−106°. Furthermore, in these isomers, the NO_2 unit is bound to the Se center trans to the $Se-N^2$ (the weakest) bond. However, in these isomers, the orientations of terminal NO-groups and location of NO_2-units relative to the Se(C_6H_4CONH) plane are different. In **2**-O(NO_2)-*cis*−*cis* and **2**-O(NO_2)-*cis*−*trans*, the NO_2 units are located on the perpendicular plane to Se(C_6H_4CONH) with their terminal N^1O^1 groups in and out position to the Se center, respectively. Therefore, in the **2**-O(NO_2)-*cis*−*cis* there is a weak N^1O^1-Se interaction, while in **2**-O(NO_2)-*cis*−*trans*, this type of interaction is absent. Meantime, in **2**-O(NO_2)-*trans*−*trans*, the NO_2 unit is located almost on the Se(C_6H_4CONH) plane with the terminal N^1O^1 group out of Se center. Interestingly, despite formation of the strong $Se=O^3$ bond, the $Se-N^2$ bonds in these products are much shorter than that in the corresponding O−O activation transition states. In other words, after O−O bond cleavage, the $Se-N^2$ bond partially recovers.

The comparison of the geometrical parameters of NO_2 units in the product complexes with those for the NO_2 and NO_2^- molecules (see Figure 1) shows that NO_2 units in **2**-O(NO_2)-*cis*−*cis*, **2**-O(NO_2)-*cis*−*trans*, and **2**-O(NO_2)-*trans*−*trans* are NO_2^- ligands. Thus, all these products are the complexes of NO_2^- anion and selenoxide OSe(C_6H_4CONH) molecule. This conclusion is consistent with the Mulliken charge analysis (see Table S3 in the Supporting Information): in these complexes, NO_2 unit has overall 0.62−0.66e negative charge. Meantime, Se center is already fully oxidized:: the positive charge on Se center is calculated to be 0.85−0.90e.

A seen in Table 1, the complexes **2**-O(NO_2)-*cis*−*cis*, **2**-O(NO_2)-*cis*−*trans*, and **2**-O(NO_2)-*trans*−*trans* are 57.0 (45.6), 56.8 (46.0), and 54.3 (42.3) kcal/mol lower than reactants and 32.8 (32.8), 25.8 (25.1), and 25.9 (25.4) kcal/mol lower than corresponding **2**-PN-*cis*−*cis*, **2**-PN-*cis*−*trans*, and **2**-PN-*trans*−*trans* complexes. These data illustrate that the product **2**-O(NO_2)-*cis*−*cis*, connected via the energetically unfavorable transition

(38) Wu, G.; Rovnyak, D.; Johnson, M. J. A.; Zanetti, N. C.; Musaev. D. G.; Morokuma, K.; Schrock, R. R.; Griffin, R. G.; Cummins, C. C. *J. Am. Chem. Soc*. **1996**, *118*, 10654 and references therein.

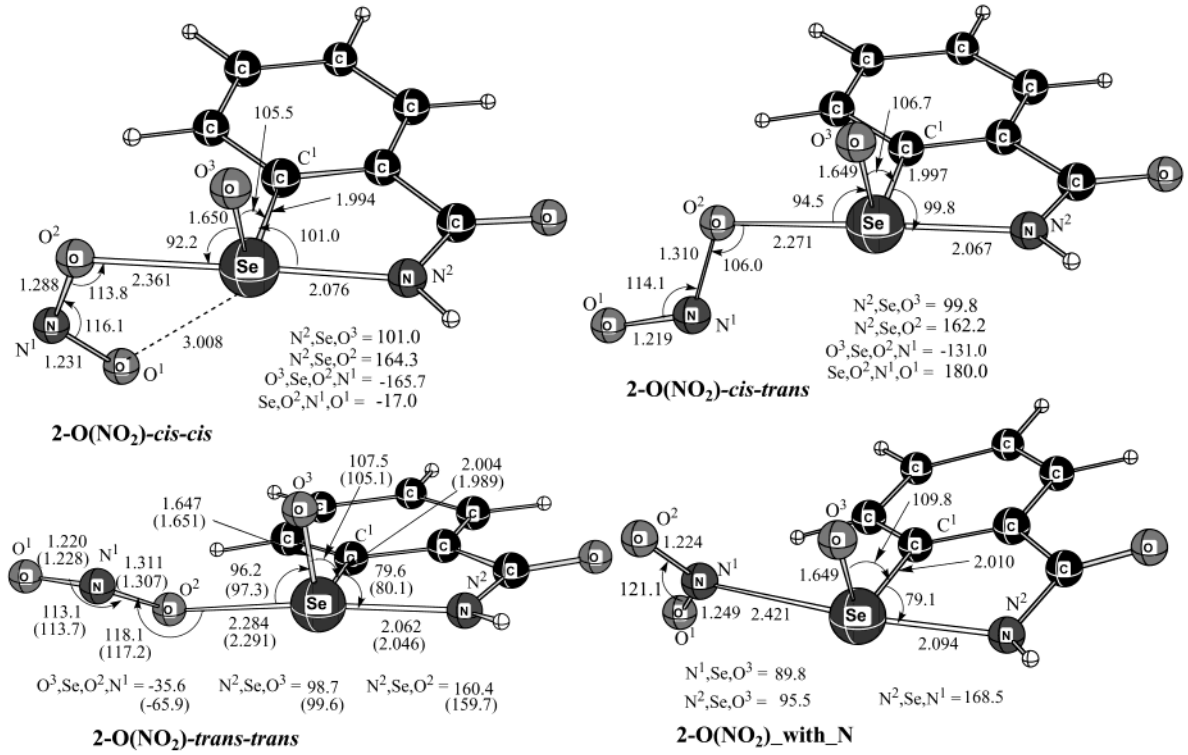

Figure 4. Calculated important geometrical parameters (distances in Å, angles in deg) of the O−O activation products, various isomers of the **2**-O(NO_2) complex. Numbers presented in parentheses were calculated at the B3LYP/6-311+G(d,p) level.

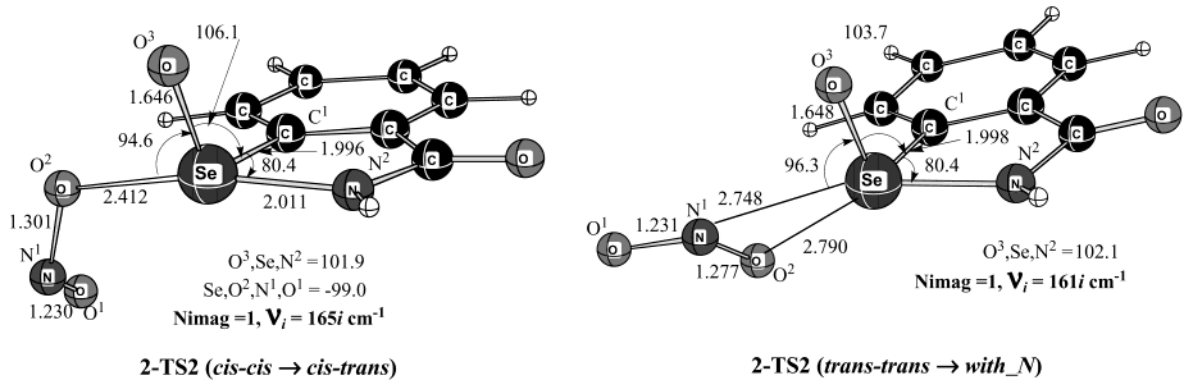

Figure 5. Calculated important geometrical parameters (distances in Å, angles in deg) of some transition states corresponding to the rearrangement of the various isomers of **2**-O(NO_2) complex.

state TS1-*cis*−*cis* to the complex **2**-PN-*cis*−*cis*, becomes most favorable product because of existence of an additional interaction between the NO_2^- fragment and the Se-center.

Thus, all these product complexes are energetically close to each other and expected to be interconnected, according to their structures presented in Figure 4. The energetic barrier connecting the complexes **2**-O(NO_2)-*cis*−*cis* and **2**-O(NO_2)-*cis*−*trans* is 4.8 (5.2) kcal/mol, calculated from the isomer **2**-O(NO_2)-*cis*−*cis*. This relatively large barrier for the **2**-O(NO_2)-*cis*−*cis* → **2**-O(NO_2)-*cis*−*trans* rearrangement could be explained in term of existence the Se−O^1 interaction in isomer **2**-O(NO_2)-*cis*−*cis*. The transition state of this process, **2**-TS2(*cis*−*cis* → *cis*−*trans*), is given in Figure 5. Another rearrangement process, transformation of **2**-O(NO_2)-*cis*−*trans* to **2**-O(NO_2)-*trans*−*trans*, is expected to follow via a simple rotational transition state around the Se−$O^2N^1O^1$ bond. Therefore, the associated barrier is not expected to be more than 1−3 kcal/mol and was not calculated.

During the studies of these rearrangement processes, we have located an additional isomer, complex **2**-O(NO_2)_with_N (depicted in Figure 4), where an NO_2 fragment coordinated to Se center via its N^1 center and cis to the Se−N^2 bond. This isomer lies 52.2 (41.1) kcal/mol lower than reactants, but 2.0 (1.2) kcal/mol higher than isomer **2**-O(NO_2)-*trans*−*trans* and separated from it with a 5.0 (4.0) kcal/mol barrier, at the transition state **2**-TS2(*trans*−*trans* → *with_N*) (Figure 5). We are aware of the existence of other isomers for **2**-O(NO_2), but we expect them to be close in energy to those that were located (see Figure 4) and separated by a small energetic barriers. Therefore, we did not locate all possible isomers and transition states for complex **2**-O(NO_2). We believe that these will not affect our conclusions.

Thus, all the isomers of **2**-O(NO_2) are energetically close and separated with reasonably low energetic barriers. Therefore, below, for simplicity, we study the important processes starting only from the lowest isomer, **2**-O(NO_2)-*cis*−*trans*.

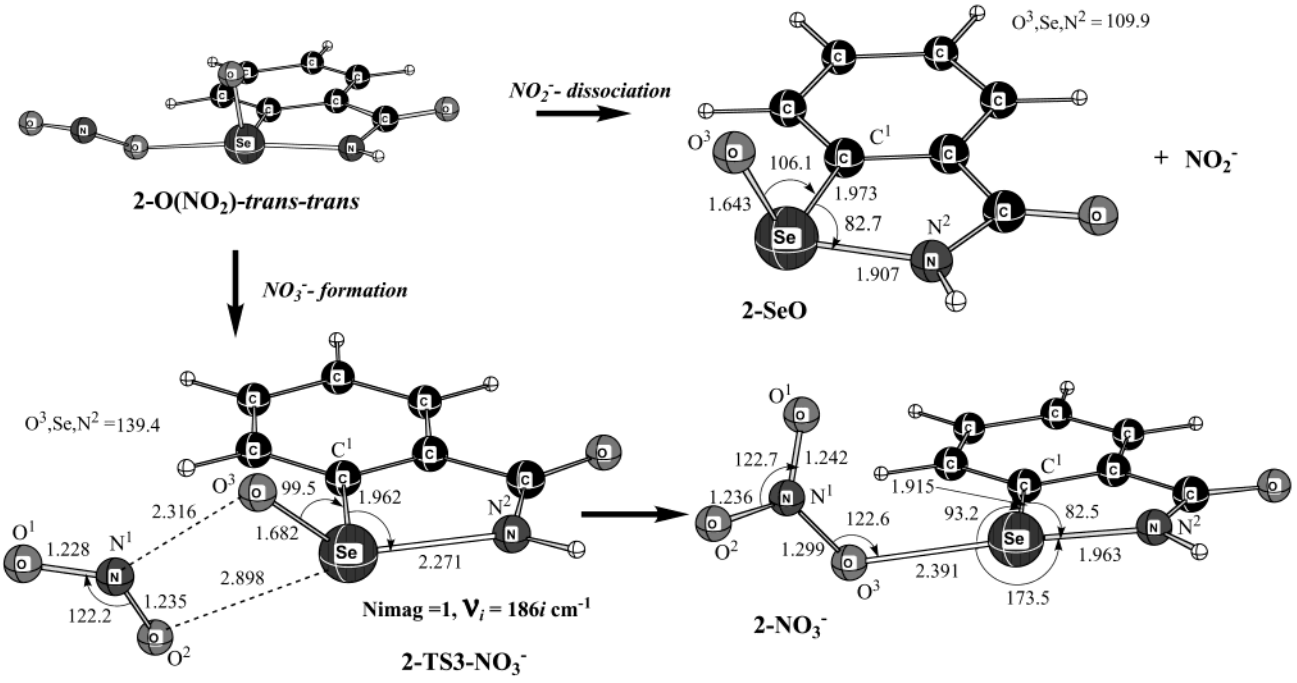

Figure 6. Calculated important geometrical parameters (distances in Å, angles in deg) of the intermediates, transition states, and products of the two different pathways, NO_2^- dissociation and NO_3^- formation, starting from the same **2**-O(NO_2)-*trans*−*trans* complex.

From the complex **2**-O(NO_2) the reaction may split into two distinct channels, NO_2^- dissociation and selenoxide formation, nitrate (NO_3^-) formation (peroxynitrite ↔ nitrate isomerization), or both. Let us discuss these processes separately.

Our calculations show that the NO_2^- dissociation from the complex **2**-O(NO_2)-*cis*−*trans* to give the experimentally observed[29] selenoxide, **2**-SeO, occurs without barrier and is endothermic by 25.3 (14.8) kcal/mol. Comparison of the values given without and with parentheses shows that the inclusion of the entropy effect reduces the endothermicity of the reaction by 10.3 kcal/mol and makes the reaction more facile (with a dissociation energy of only 14.8 kcal/mol). The final products **2**-SeO + NO_2^- lie 31.5 (31.2) kcal/mol lower than reactants **2** + PN. As seen in Figure 6, dissociation of NO_2^- results in complete recovery of Se−N^2 bond: the calculated Se−N^2 bond distance is 1.907 Å in **2**-SeO, which is close to that, 1.876 Å, in the reactant **2**.

The second process starting from the **2**-O(NO_2) complex is NO_3^- formation, which occurs via transition state **2**-TS3−NO_3^-, given in Figure 6. Our normal-mode analysis shows that this is a real transition state with one imaginary frequency of 186i cm^{-1} corresponding to the formation of the N^1−O^3 bond. The N^1−O^3 bond distance in **2**-TS3−NO_3^- is calculated to be 2.316 Å, which is significantly smaller than that in prereaction complex **2**-O(NO_2)-*trans*−*trans*, 3.223 Å. Meantime, the Se−O^3 bond distance in **2**-TS3−NO_3^- is elongated by 0.035 Å compared with that in the prereaction complex **2**-O(NO_2)-*trans*−*trans*. These data show that the transition state **2**-TS3−NO_3^- is a relatively early transition state, where the important geometrical parameters are closer to those in the prereaction complex. IRC calculations show that the **2**-TS3−NO_3^- connects complex **2**-O(NO_2)-*trans*−*trans* with the product **2**-NO_3^-, given in Figure 6.

The barrier height at the transition state **2**-TS3−NO_3^- is 22.9 (22.7) kcal/mol calculated from the complex **2**-O(NO_2)-*cis*−*trans*.

In the resulting complex **2**-NO_3^-, the NO_3^- ligand is already formed and coordinated to the Se center of **2** with one of its O-atoms, O^3 (see Figure 6). The calculated Se−O^3 bond distance is 2.391 Å. Meantime, the calculated Se−N^2 bond distance in **2**-NO_3^-, 1.963 Å, which is slightly shorter than that in **2**-O(NO_2)-*trans*−*trans*, 2.062 Å, indicating that NO_3^- is a weaker trans ligand than NO_2^-. Indeed, the calculations show that Se−NO_3^- binding energy in **2**-NO_3^- is 19.6 (8.8) kcal/mol versus 25.3 (14.8) kcal/mol Se−NO_2^- binding energy in **2**-O(NO_2)-*cis*−*trans*. Complex **2**-NO_3^- is calculated to be about 16.5 (15.0) kcal/mol more stable than the lowest (cis−trans) isomer of the prereaction complex **2**-O(NO_2). Thus, the entire process, **2** + PN → **2** + NO_3^- is found to be exothermic by 52.7 (52.2) kcal/mol. These numbers are the peroxynitrite → nitrate isomerization energies.

Overall potential energy surface of the reaction **2** + PN in the gas phase is presented in Figure 7. As seen from this figure, the reaction **2** + PN is highly exothermic. It starts with coordination of PN to Se center, which is exothermic by 31.0 (20.9) kcal/mol. Then, the resulting intermediate converts to **2**-O(NO_2) via O−O bond cleavage barrier of 6.0 (7.7) kcal/mol. The complex **2**-O(NO_2) is a (NO_2^-)-**2**-SeO type of complex, which has several isomers that can easily rearrange to each other. The lowest energy isomer, the cis−trans isomer, lies about 56.8 (46.0) and 25.8 (25.1) kcal/mol lower than the reactants, **2** + PN and the lowest energy isomer of **2**-PN, respectively. Thus, the reaction **2** + PN → **2**-O(NO_2) is believe to be very fast in the gas phase.

The processes starting from the complex **2**-O(NO_2) are rate-determining steps of the entire **2** + PN reaction and may lead to two different sets of final products. One of them, the NO_2^- dissociation and selenoxide formation reaction, was experimentally reported[29] to proceed extremely fast at alkaline pH. Our calculations performed in the gas phase show that entire reaction **2** + PN → **2**-SeO + NO_2^- is exothermic by 31.5 (31.2) kcal/

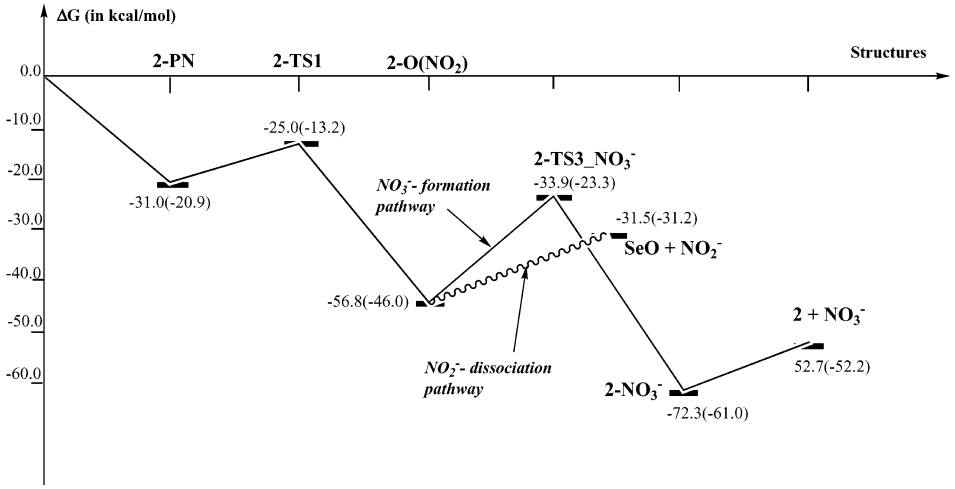

Figure 7. Schematic representation of potential energy surface of the reaction **2** + PN, calculated at the B3LYP/6-311+G(d,p)//B3LYP/6-311G(p,d) level. Here, we have presented energies of only the lowest possible isomers of calculated intermediates and transition states. The numbers outside the parentheses are ΔH values, while those inside the parentheses are ΔG values.

mol, while its final step, **2**-O(NO_2) → **2**-SeO + NO_2^-, is endothermic by 25.3 (14.8) kcal/mol.

Meantime, the second process, nitrate formation, takes place with 22.9 (22.7) kcal/mol barrier at the transition state **2**-TS3−NO_3^-**.** The resulting **2**-NO_3^- complex lies 16.5 (15.0) kcal/mol lower than the lowest (cis−trans) isomer of the prereaction complex **2**-O(NO_2). The last step of this path, **2**-NO_3^- → **2** + NO_3^-, is found to be endothermic by 19.6 (8.8) kcal/mol. The entire process, **2** + PN → **2** + NO_3^- is exothermic by 52.7 (52.2) kcal/mol.

Thus, the rate-determining step of the nitrate formation process, the kinetic barrier at the transition state **2**-TS3−NO_3^-, calculated from the complex **2**-O(NO_2)-*cis*−*trans* is (22.7) kcal/mol, including zero-point energy, temperature, and entropy corrections. This value is significantly (7.9) kcal/mol larger than the rate-determining step (14.8) kcal/mol of the NO_2^- dissociation pathway starting from the same complex **2**-O(NO_2)-*cis*−*trans*. Therefore, the nitrate formation process is unlikely to compete with the NO_2^- dissociation process. In other words, *the products of the reaction* ***2*** *+ PN will be* NO_2^- *and selenoxide, even in the gas phase. Thus, the peroxynitrite → nitrate isomerization catalyzed by complex* ***2*** *is unlikely.*[39]

Furthermore, the analysis of the important geometrical parameters along the potential energy surface (PES) of the reaction **2** + PN shows that the Se−N^2 bond is very flexible and significantly changes during the reaction, thus facilitating it. In the first step of the reaction, coordination of PN to **2**, the Se−N^2 bond elongates, which is crucial for formation of the strong Se−PN bond. In the next step, O^3−O^2 cleavage, the Se−N^2 bond elongates further to facilitate Se−O^3 bond formation and, consequently, O^3−O^2 bond cleavage. Most likely in the close vicinity of the O^3−O^2 cleavage transition state the reorganization of geometrical parameters, especially movement of the Se−O^3 bond from the trans to cis with respect to the Se−N^2, occurs and results in the partial recovering of Se−N^2 bond. This in turn, increases the overall exothermicity of the reaction **2**-PN-*cis*−*trans* → **2**-O(NO_2)-*cis*−*trans*. In the last stage of the reaction, the dissociation of NO_2^- and formation **2**-SeO, the Se−N^2 bond almost fully recovers and reduces the endothemicity of this step of the reaction. On the basis of these observations, one may predict that ebselen derivatives are similar to **2**, but with no Se−N^2 bond, will be extremely active in the first part of the reaction, i.e., for the PN coordination and O−O bond activation. At the same time, ebselen derivatives such as **2**, but with a strong Se−N^2 bond, will be extremely desirable for the final step of the reaction, the dissociation of NO_2^- and formation of **2**-SeO complex.

In addition, the Se−N^2 bond distance significantly elongates at the transition state **2**-TS3−NO_3^- compared with the pre reaction complex **2**-O(NO_2)-*trans*−*trans* and facilitates the reaction. Therefore, one could expect that catalysts similar to complex **2**, but with a weak, or nonexistent, Se−N^2 bond, will facilitate the NO_3^- formation process. However, having a weak, or nonexistent, Se−N^2 bond in the reactant complex may hamper the final step, NO_3^- dissociation, which is expected to be easier for the complexes with strong Se−N^2 bonds.

In summary, *one may expect that the ebselen derivatives with nonexistent* (*or extremely weak*) *Se*−N^2 *bonds* (*or any Se*−*X bond, where X is bound to the* N^2 *center*) *may facilitate the peroxynitrite → nitrate isomerization process.*

Testing these ideas and predicting the ebselen derivatives that could make feasible peroxynitrite → nitrate isomerization will be the subject of our independent studies. But below, we would like to partially check the above presented ideas and elucidate the roles of electronic effects in the rate-determining steps of NO_2^- dissociation and NO_3^- formation. For these purposes, we have replaced the H ligand bound to N^2 by the electron-withdrawing CH_3, C_6H_5, and CF_3 and electron-donating $OSiH_3$, OH, and NH_2 groups (see Scheme 1).

Elucidating the Role of Electronic Effects in the NO_2^- Dissociation and NO_3^- Formation Processes. Now let us address the effects of the more electron-withdrawing CH_3, C_6H_5, and CF_3, and electron-donating $OSiH_3$, OH, and NH_2 groups on the energetics and geometries of the complexes ***n***-O(NO_2)-*cis*−*trans*, the transition states ***n***-TS3−NO_3^-, and the products ***n***-SeO + NO_2^-**.** The calculated relative energies and important geometrical parameters of these structures are given in Tables

(39) Since the dissociation of **2**-O(NO_2) to NO_2^- and selenoxide is endothermic and its isomerization to **2**-(NO_3^-) requires large energetic barrier in the gas-phase, one may expect the formation of **2**-O(NO_2) as a final product.

Table 2. Energies (in kcal/mol, Relative to the 2-O(NO_2)-*cis*−*trans*) of the Rate-Determining Steps for NO_2^- Dissociation and NO_3^- Formation Pathways Calculated for Different R (R═H, CH_3, CF_3, C_6H_5, $OSiH_3$, OH, and NH_2) (see Chart 1)[a]

structures	**2**, H	**3**, CH_3	**1**, C_6H_5	**4**, CF_3	**5**, $OSiH_3$	**6**, OH	**7**, NH_2
n−O(NO_2)-*cis*−*trans_1*	0.0	0.0	0.0	0.0(0.0	0.0	0.0(0.0)	0.0
n-TS3_NO_3	23.8	23.6	21.4	20.6(19.2)	19.5	18.9(18.5)	22.4
n-SeO + NO_2^-	26.4	25.6	29.5	35.4(22.5)	28.7	31.2(19.2)	25.9
Δ[2-TS3_NO_3 − (2-SeO + NO_2^-)]	−2.6	−2.0	−8.1	−14.8(−3.3)	−9.2	−12.3(−0.7)	−3.5

[a] All numbers were obtained at the B3LYP/6-311+G(d,p)//B3LYP/6-311G(d,p) level and do not include the zero-point energy and entropy corrections except those (in parentheses) for R═CF_3 and OH.

Table 3. Calculated Important Bond Distances (in Å) of the Crucial Structures of the NO_2^- Dissociation and NO_3^- Formation Pathways for Different R (R═H, CH_3, CF_3, C_6H_5, $OSiH_3$, OH, and NH_2) (see Chart 1)[a]

structures	parameters	**2**, H	**3**, CH_3	**1**, C_6H_5	**4**, CF_3	**5**, $OSiH_3$	**6**, OH	**7**, NH_2
n-O(NO_2)-*cis*−*trans*	Se−N^2	2.062	2.068	2.179	2.244	2.096	2.180	2.097
	Se−C^1	2.004	1.991	1.980	2.001	1.995	2.005	1.995
	Se−O^3	1.647	1.652	1.648	1.637	1.659	1.642	1.647
	Se−O^2	2.284	2.264	2.179	2.171	2.196	2.208	2.235
	O^3-N^1	3.223	3.711	3.567	3.159	3.614	3.681	3.626
n-TS3_NO_3	Se−N^2	2.271	2.274	2.422	2.349	2.456	2.453	2.337
	Se−C^1	1.962	1.955	1.945	1.968	1.946	1.965	1.965
	Se−O^3	1.682	1.683	1.671	1.644	1.669	1.666	1.678
	O^3-N^1	2.316	2.327	2.369	2.374	2.365	2.473	2.348
n-SeO	Se−N^2	1.907	1.915	1.940	1.965	1.968	1.976	1.940
	Se−C^1	1.973	1.965	1.959	1.963	1.961	1.976	1.965
	Se−O^3	1.643	1.646	1.646	1.636	1.640	1.642	1.642

[a] All numbers presented here were obtained at the B3LYP/6-311G(d,p) level.

2 and 3, respectively, for ***n*** = **1**−**7**. Note that the relative energies given in Table 2 do not include the zero-point energy and entropy corrections except for R═CF_3 and OH. Therefore, here, the numbers given without parentheses are Δ*E* values rather than enthalpies. We believe that the discussion of Δ*E* values will not affect our final conclusions because they are very close to the corresponding Δ*H* values (see Table 1).

As seen from Table 2, the energy difference, Δ, between the rate-determining steps of NO_2^- dissociation and NO_3^- formation, which are the NO_2^- dissociation energy from the complex ***n***−O(NO_2)-*cis*−*trans* and the energy barrier at the transition states ***n***-TS−NO_3^-, respectively, increases with increasing electron-withdrawing nature of the R group, i.e., via H (2.6) ≈ CH_3 (2.0) < C_6H_5 (8.1) < CF_3 (14.8). The increasing electron-withdrawing nature of the R group strongly destabilizes the ***n***-SeO + NO_2^- dissociation limit, while it slightly stabilizes ***n***-TS−NO_3^- (there is destabilization in the case R═CH_3). As a result, Δ increases, and consequently, the feasibility of the NO_3^- formation process increases. Most promising is complex **4** with the strongest electron-withdrawing ligand R═CF_3, for which we also evaluated the zero-point energy, temperature, and entropy corrections, ΔΔ, at the B3LYP/6-311G(d,p) level and added to the final B3LYP/6-311+G(d,p) energetics. As seen in Table 2, the NO_3^- formation process even after including ΔΔ, is slightly (3.3 kcal/mol) more favorable than the NO_2^- dissociation process *indicating that **4** could be a good catalyst for peroxynitrite ↔ nitrite isomerization in the gas phase.*

Table 3, where we have presented the calculated important bond distances, shows that the trend in the energetics noted above agrees well with the calculated Se−N^2 bond distance in the prereaction complex ***n***−O(NO_2)-*cis*−*trans* and product ***n***-SeO, which, in general, increases as R═H < CH_3 < C_6H_5 < CF_3. *Thus, the weaker Se−N^2 bond, the larger the NO_2^- dissociation energy, as predicted above.* However, there are no well-defined trends in the geometries of the transition states ***n***-TS−NO_3^-.

Similar trends were obtained for the derivatives of **2** with electron-donating groups, NH_2, $OSiH_3$, and OH: Δ increases as H (2.6) < NH_2 (3.5) < $OSiH_3$ (9.2) < OH (12.3). This trend in energetics correlates well with the calculated Se−N^2 bond distances, which increase as NH_2 < $OSiH_3$ < OH. Thus, among these catalysts, **6**, with R═OH, looks most promising. Even after including zero-point energy and entropy corrections, the NO_3^- formation process is slightly (0.7 kcal/mol) more favorable than the NO_2^- dissociation process. Thus, *complex **6** could catalyze the peroxynitrite ↔ nitrite isomerization in the gas phase.*

Role of Solvent Effects. Here, we divide our discussions into two parts. First, we discuss the effects of solvent on the calculated relative energies of the reactants, intermediates, transition states, and products of reaction **2** (R═H) with PN. Second, we elucidate the roles of solvent molecules in the important steps of reaction **4** (R═CF_3) with PN, because complex **4** is predicted to be a good catalyst for the peroxynitrite ↔ nitrate isomerization process in the gas phase. In these calculations, we use water, dichloromethane, benzene, and cyclohexane as the solvent. Note that the single-point PCM calculations provide the value called delta*G*(solution), which does not include zero-point energy and entropy corrections, ΔΔ, and could be compared only with Δ*E* value for the gas phase. Therefore, below it will be called Δ*E* solution. To include zero-point energy and entropy corrections, one has to optimize geometries and recalculate the frequencies of each structure in the solution phase. However, these types of calculations are unavailable. Therefore, we have calculated ΔΔ in the gas phase and added this to delta*G*(solution). The final quantity is called Δ*G*, because it could be compared with relative Gibbs free energies for the gas phase. Note, previously it was demonstrated[40] that this type of approach is reasonably accurate and does not influence the final conclusions. The data presented below for the peroxynitrite ↔ nitrate isomerization energy

(40) Szilagyi, R. K.; Musaev, D. G.; Morokuma, K. *Organometallics* **2002**, *21*, 555 and references therein.

Table 4. Relative Energies (in kcal/mol) of the Intermediates, Transition States, and Products of the Reaction **2** + PN, in the Gas Phase and in Water, Dichloromethane, Benzene, and Cyclohexane Solutions

	gas phase		H_2O		CH_2Cl_2		C_6H_6		C_6H_{12}	
structures[b]	ΔE	ΔG	ΔE[c]	ΔG[d]	ΔE	ΔG	ΔE	ΔG	ΔE	ΔG
$OONO^-$, cis	0.0	0.0	0.0	0.0	0.0	0.0	0.0	0.0	0.0	0.0
$OONO^-$, ts	27.1	25.8	24.5	23.2	25.6	24.3	26.5	25.2	26.6	25.3
$OONO^-$, trans	3.4	3.1	4.8	4.5	4.3	4.1	3.9	3.6	3.9	3.6
2 + *cis*-$OONO^-$	0.0	0.0	0.0	0.0	0.0	0.0	0.0	0.0	0.0	0.0
2-PN-*cis*−*cis*	−25.3	−12.8	0.4	12.9	−6.9	5.6	−14.0	−1.5	−14.4	−1.9
2-PN-*cis*−*trans_1*	−32.2	−20.9	−6.3	5.0	−12.2	−0.9	−20.0	−8.7	−20.6	−9.3
2-PN-*trans*−*trans_1*	−29.5	−16.9	−3.1	9.5	−9.1	3.5	−17.1	−4.5	−17.6	−5.0
2-TS1-*cis*−*cis*	−11.5	0.6	11.8	23.9	5.0	17.1	−1.1	11.0	−1.7	10.4
2-TS1-*cis*−*trans*	−25.1	−13.2	2.0	13.9	−4.4	7.5	−12.2	−0.3	−13.0	−1.1
2-TS1-*trans*−*trans*	−20.8	−9.4	4.2	15.6	−1.0	4.2	−8.5	2.9	−9.2	2.2
2-O(NO_2)-*cis*−*cis*	−58.2	−45.6	−40.7	−28.6	−42.8	−30.2	−48.3	−35.7	−49.0	−36.4
2-O(NO_2)-*cis*−*trans*	−58.0	−46.0	−39.7	−27.7	−42.1	−30.1	−47.9	−35.9	−48.5	−36.5
2-O(NO_2)-*trans*−*trans*	−55.7	−42.3	−38.5	−25.1	−40.3	−26.9	−45.7	−32.3	−46.4	−33.0
2-O(NO_2)_*with_N*	−53.7	−41.1	−35.2	−22.6	−37.6	−25.0	−43.2	−30.6	−43.7	−31.1
2-TS2(*cis*-*cis*→ *cis*−*trans*)	−52.7	−40.4	−33.5	−21.1	−37.0	−24.7	−42.3	−30.0	−43.2	−30.9
2-TS3_ NO_3^-	−34.2	−23.3	−12.8	−1.9	−15.9	−5.0	−22.5	−11.6	−23.2	−12.3
2-NO_3^-	−74.9	−61.0	−52.2	−38.3	−56.7	−42.8	−63.7	−49.8	−64.2	−50.3
2 + NO_3^-	−54.2	−52.2	−51.5	−49.5	−53.3	−51.3	−53.9	−51.9	−53.9	−51.9
2-SeO + NO_2^-	−31.6	−31.2	−37.1	−36.7	−35.7	−35.3	−33.9	−33.5	−33.8	−33.4

[a] All numbers presented here were calculated at the B3LYP/6-311+G(d,p)//B3LYP/6-311G(d,p) (for gas phase) and PCM- B3LYP/6-311+G(d,p)//B3LYP/6-311G(d,p) (for solution) levels of theory. [b] Structures given in Figures 1−6. [c] PCM calculations provide the value called delta*G*(solution), which does not include zero-point energy and entropy corrections, $\Delta\Delta$ (see Table 1), and could be compared only with ΔE value for the gas phase. Therefore, here it is called ΔE for solution. [d] $\Delta G = \Delta E + \Delta\Delta$. Here, the $\Delta\Delta$ calculated at the gas phase and added to delta*G*(solution). The final quantity is called ΔG, because it could be compared with relative Gibbs free energies for the gas phase (see text for more details).

Table 5. Relative Energies (in kcal/mol) of the Important Intermediates, Transition States, and Products of Reaction **4** + PN, in the Gas Phase and in Water, Dichloromethane, Benzene, and Cyclohexane Solutions

	gas phase		water		CH_2Cl_2		C_6H_6		cyclohexane	
structures	ΔE	ΔG	ΔE	ΔG	ΔE	ΔG	ΔE	ΔG	ΔE	ΔG
4-O(NO_2)-*cis*−*trans*	0.0	0.0	0.0	0.0	0.0	0.0	0.0	0.0	0.0	0.0
4-TS3_NO_3^-	23.8	22.7	19.4	18.3	20.7	19.6	20.9	19.8	20.9	19.8
4-SeO + NO_2^-	26.4	14.8	4.4	−7.2	11.7	0.1	14.7	3.1	15.2	3.6
Δ[**2**-TS3_NO_3^- − (**2**-SeO + NO_2^-)]	−2.6	7.9	15.0	25.5	9.0	19.5	6.2	16.7	5.7	16.2

[a] All numbers presented here were calculated at the B3LYP/6-311+G(d,p) //B3LYP/6-311G(d,p) (for gas phase) and PCM- B3LYP/6-311+G(d,p) //B3LYP/6-311G(d,p) (for solution) levels of theory.[a] See footnotes of Table 5 for explanations of ΔE and ΔG.

calculated in water and compared with its experimental value indicate that the accuracy of this type of approach is within 3−5 kcal/mol.

In Table 4 we have presented the calculated relative energies for the reaction **2** + PN. Since the largest contributions from the solvent to the calculated energetics are electrostatic terms, one may expect that solvent effects will be significant at the beginning, **2** + $OONO^-$ and also at the end, **2**-SeO + NO_2^- and **2** + NO_3^-, of the reaction. Indeed, the calculations show that including solvent effects dramatically (up to 26 kcal/mol) reduces the $ONOO^-$ complexation, as well as the NO_2^- and NO_3^- dissociation energies, and these effects increase with increasing solvent polarity. In the most polar solvent, water, the coordination of PN to **2** becomes endothermic and the O−O activation step, which was not rate-determining in gas phase, becomes rate determining for the overall reaction. The calculated the O−O bond activation transition state lies about 13−14 kcal/mol higher in energy than the reactants, **2** + PN. In the relatively nonpolar solvents (benzene and cyclohexane), this transition state is still lower in energy than the reactants and can proceed relatively fast (with barriers of 7.8 (8.4) and 7.6 (8.2) kcal/mol, respectively). Even in these nonpolar solvents, the O−O activation step becomes a rate-determining step of the reaction. Furthermore, since solvent effects significantly reduce the NO_2^- dissociation energy, while only slightly destabilizing the NO_3^- formation barrier at **2**-TS3−NO_3^- (calculated from **2**-O(NO_2)-*cis*−*trans*), the peroxynitrite ↔ nitrate isomerization process becomes impossible in solution, and therefore, the only direct products of the reaction **2** with PN are going to be nitrite and selenoxide molecules.

Similar solvent effects were found for the important steps, the NO_2^- dissociation and the NO_3^- formation, of the reaction of **4** with PN. Because of strong stabilization of the NO_2^- dissociation process by solvent, even for the reaction **4** + PN, the peroxynitrite ↔ nitrate isomerization process, in spite being favorable in the gas phase, becomes impossible in solution.

As seen in Table 5, the calculated peroxynitrite ↔ nitrate isomerization energy in gas phase, water, dichloromethane, benzene, and cyclohexane, are 54.2 (52.2), 51.5 (49.5), 53.3 (51.3), 53.9 (51.9), and 53.9 (51.9) kcal/mol, respectively, where numbers without the parentheses are ΔE values. The values obtained in aqueous solution, 51.5 (49.5) kcal/mol, are in reasonable agreement with the available experiment data for Gibbs free energy of peroxynitrite ↔ nitrate isomerization, 40−43 kcal/mol.[41]

Conclusions

From above presented discussions one may draw the following conclusions:

1. The reaction of **2** with PN proceeds via **2** + PN → **2**-PN → **2**-TS1 (O−O activation) → **2**-O(NO_2^-) → **2**-SeO + NO_2^- with a rate-determining barrier of 25.3 (14.8) kcal/mol for the NO_2^- dissociation step at the gas phase. The direct products of this reaction are NO_2^- anion and selenoxide. This conclusion is in agreement with available experiment.[29]

2. The second possible process, NO_3^- formation, starting from the **2**-O(NO_2^-) complex, requires (7.9) kcal/mol more energy than NO_2^- dissociation and is unlikely to compete with the latter. Thus, in gas phase, the peroxynitrite → nitrate isomerization catalyzed by complex **2** is unlikely to occur.

3. The Se−N^2 bond is found to be extremely flexible. It changes significantly during the reaction and facilitates the reaction. The ebselen derivatives with nonexistent (or weak) Se−N^2 bonds are predicted to be active for the PN coordination and the O−O bond acleavage steps, as well as for the nitrate formation process. Meantime, the ebselen derivatives with strong Se−N^2 bond are predicted to be useful for the NO_2^- dissociation and selenoxide formation.

4. The energy difference, Δ, between the rate-determining steps of NO_2^- dissociation and NO_3^- formation increases with increasing electron-withdrawing ability of the group R, in the order H (2.6) ≈ CH_3 (2.0) < C_6H_5 (8.1) < CF_3 (14.8). The NO_3^- formation process is slightly (3.3 kcal/mol) more favorable than the NO_2^- dissociation process for the compound with the strongest electron-withdrawing group R═CF_3, **4**. We predict that **4** could be a good catalyst for peroxynitrite ↔ nitrite isomerization in the gas phase. Another promising catalyst for the peroxynitrite ↔ nitrite isomerization in gas phase is predicted to be the complex **6** (R═OH).

5. Solvent effects changes the rate-determining step of the reaction of **2** + PN. O−O activation becomes rate determining with barriers of 8.3 (13.9), 7.8 (8.4), 7.8 (8.4), and 7.6 (8.2) kcal/mol in water, dichloromethane, benzene, and cyclohexane, respectively. Furthermore, since solvent effects significantly reduce the NO_2^- dissociation energy, while only slightly destabilizing the NO_3^- formation barrier, the peroxynitrite ↔ nitrate isomerization becomes practically impossible in solution, even for complex **4**. Therefore, the formation of nitrate during the reaction of complexes **1**−**7** with PN is unlikely.

Acknowledgment. D.G.M. acknowledges the Visiting Professorship from the University of Tokyo, Japan. Acknowledgment is also made to the Cherry L. Emerson Center of Emory University for the partial use of its resources, which is in part supported by a National Science Foundation grant (CHE-0079627) and an IBM Shared University Research Award.

Supporting Information Available: The *x*, *y*, *z* coordinates of all calculated reactants, intermediates, transition states, and products of the reaction **2** + PN (Table S1); their total energies (Table S2**)** and Mulliken charges (Table S3); the *x*, *y*, *z* coordinates all calculated important structures of the reaction of complexes **1**−**7** with PN (Table S4**)**; their total energies (Table S5**)**; Mulliken charge analysis (Table S6**)** of important structures of the reaction of **1**−**7** with PN; calculated Delta**G**(solvation) values at the PCM level for all reactants, intermediates, transition states, and products of the reaction **2** + PN (Table S7) and **4** + PN (Table S8). This information is available free of charge via the Internet at http://pubs.acs.org.

JA0286324

(41) Calculations are based on $\Delta_f G°$ (NO_3^-) = −26.6 kcal/mol, and $\Delta_f H°$ (NO_3^-) = −49.6 kcal/mol (see: *CRC Handbook of Chemistry and Physics*; Lide, D. R., Frederikse, H. P. R., Eds.; CRC Press: Boca Raton, FL, New York, 1996); $\Delta_f G°$ ($ONOO^-$) = 16.4 kcal/mol (see: Goldstein, S.; Czapski, G.; Lind, J.; Merenyi, G. *Chem Res. Toxicol.* **2001**, *14*, 657); and 14±3 kcal/mol (see: Koppenol, W. H.; Kissner, R. *Chem Res. Toxicol.* **1998**, *11*, 87).